Spectrum Simulation of Li-Like Aluminium Plasma *

PENG Feng(彭枫)[1,2], JIANG Gang(蒋刚)[2**], ZHU Zheng-He(朱正和)[2]

[1]*Department of Physics and Electronic Technology, Luoyang Normal College, Luoyang 471022*
[2]*Institute of Atomic and Molecular Physics, Sichuan University, Chengdu 610065*

(Received 17 July 2006)

X-ray emission spectra for L-shell of Li-like aluminium ions are simulated by using the flexible atomic code based on the collisional radiative model. Atomic processes including radiative recombination, dielectronic recombination, collisional ionization and resonance excitation from the neighbouring ion (Al^{9+} and Al^{11+}) charge states of the target ion (Al^{10+}) are considered in the model. In addition, the contributions of different atomic processes to the x-ray spectrum are analysed. The results show that dielectronic recombination, radiative recombination, collisional ionization and resonance excitation, other than direct collisional excitation, are very important processes.

PACS: 32. 30. Rj, 52. 25. Tx

X-ray spectroscopy of plasmas has been received much attention over the past few years due to its extensive applications in exploding wire experiments,[1,2] laser plasmas,[3,4] particle beam-foil interactions,[5] radiative opacity,[6] astrophysics, and plasma diagnostics.[7−10] Theoretical analyses of emission from these plasmas are of great use for understanding the plasmas energetics and the determination of plasmas parameters. Several models concentrating on K-shell ions,[11] L-shell ions,[12] and M-shell ions[13] have been developed to understand various aspects of aluminium plasma emission.

The collisional radiative model (CRM) in the flexible atomic code (FAC)[14] is established to gain the x-ray spectrum of Li-like Al plasma, which reflects the properties such as temperature and density. To obtain the correct spectrum, the determined collisional and radiative processes such as collisional ionization (CI), radiative recombination (RR) and collisional excitation (CE) as well as two-electron processes such as autoionization (AI) and dielectronic recombination (DR) are considered in the model. Three ions, i.e. target ion Al^{10+} and the neighbouring ions (Al^{11+} and Al^{9+}), are involved in the systematic equilibrium and the equilibrium of the three ions dynamics processes can be presented sententiously as follows:

$$\mathrm{Al}^{11+}(\mathrm{CE}) \underset{\text{CI, AI}}{\overset{\text{DR, RR}}{\rightleftharpoons}} \mathrm{Al}^{10+}(\mathrm{CE}) \underset{\text{CI, AI}}{\overset{\text{DR, RR}}{\rightleftharpoons}} \mathrm{Al}^{9+}(\mathrm{CE}).$$

In this Letter, we employ the CRM to simulate x-ray spectrum emission from Li-like aluminium plasma and to calculate the population and rate coefficients. The relations among x-ray wavelengths, relatively radiative intensity and the electronic temperature are obtained, which are important for plasmas diagnostics.

The corona equilibrium model, generally used for CI, only includes CE from the ground state of each ion and the subsequent radiative cascades. Therefore, the spectra for different charge states can be treated separately. Since the neighbouring charge states of the target ion are involved in the indirect processes, the rate equations governing the statistical equilibrium, which include atomic states from multiple ions, can be written as

$$\sum_{ij} C_{pi}^{qj} n_{qj} = 0, \tag{1}$$

where n_{qj} is the population of level j in ion q. If $q \neq p$ or $i \neq j$, C_{pi}^{qj} is the total rate of the populating of state pi by qj, if $q = p$ and $i = j$, $C_{pi}^{qj} = -D_{pi}$, where D_{pi} is the total depletion rate of state pi, and D_{pi} can be presented as follows:

$$D_{pi} = \sum_{qj \neq pi} C_{pi}^{qj}. \tag{2}$$

It is noted that Eq. (1) is homogeneous and does not provide a unique solution, the normalization condition is

$$\sum_{qj} n_{qj} = 1 \tag{3}$$

which needs to be incorporated with Eq. (1). For the single-ion model, the normalization condition is used to fix the total density of the ions. For the multi-ion model, a self-consistent solution with such normalization condition simultaneously yields the ionization equilibrium and the level population for each ion. However, all the important ionization and recombination channels of all charge states are needed to be included in Eq. (1), which is impractical and unnecessary. The ionization equilibrium can be calculated separately without considering the detailed level population for each ion. Namely, instead of all ions of the atomic elements, the normalization condition can be applied for each ion,

$$\sum_{j} n_{qj} = n_q, \tag{4}$$

* Supported by the National Defence Foundation of China under Grant No 51480020204SC0102.
** To whom correspondence should be addressed. Email: gjiang@scu.edu.cn
©2006 Chinese Physical Society and IOP Publishing Ltd

where n_q is the fractional abundance of ion q obtained from a separate ionization balance calculation, or equivalently, one can set $C_{p0}^{qj} = 1$ for all p, $C_{p0}^{qj} = 0$ for $q \neq p$, and replace the right side on Eq. (1) with a vector

$$b = [n_0, 0, \ldots, n_q, 0 \ldots]^T, \tag{5}$$

which makes Eq. (1) inhomogeneous and therefore yields a unique solution. The intensity of a line produced by radiative decay from state pi to pj is obtained by

$$I_{ij}^P = AN_H n_{pi} A_{pj}^{pi}, \tag{6}$$

where A is the elemental abundance relative to hydrogen, N_H is the hydrogen density, and A_{pj}^{pi} is the radiative decay rate (Einstein A-coefficient) from the state pi to pj.

Since the number of double-excited states producing dielectronic recombination (DR) and resonance excitation (RE) far exceeds those directly responsible for line emission, the solution of the rate equations can not be gained with the standard procedures. A reduced atomic model[15] is introduced, in which instead of solving the original rate equations, a reduced atomic model is constructed by grouping a large number of atomic states in a so-called superlevel. Specifically, in this code, states from the same complex and the same ion are grouped to form a superlevel except for a few tens of the lowest lying levels, where a superlevel contains only one real state. For example, excited states of n-manifold and resonance states of $nln'l'$ type are grouped into separate superlevels. The density of the superlevel is defined as

$$n_{pJ} = \sum_j n_{pj}, \tag{7}$$

where the summation is over the states forming the superlevel J and the coefficients C_{pI}^{qJ} are given as

$$C_{pI}^{qJ} = \sum_{ij} C_{pi}^{qj} n_{qj}, \tag{8}$$

where the summation over i and j includes all the states forming superlevels I and J, respectively. With these definitions, if the original rate equations are satisfied, the similar equations are for the reduced atomic model and the solution of Eq. (1) can also be achieved iteratively. In this work, the iteration is terminated when the difference between the level populations in two consecutive steps is within 10^{-4}.

Before discussing the contributions of individual processes to the line formation, we compared the total recombination and ionization rate coefficients obtained in this work with previous publications. Figure 1 shows the total DR rate coefficients of the present calculation together with the results of Mazzotta (1998) (hereafter M98)[16] and Colgan *et al.* (2004) (C04)[17] for Al^{10+}. The present DR rate coefficients agree with those of M98 in lower electron temperature ($T = 10^4$–10^7 K), fit with those of C04 in higher temperature ($T = 10^6$–10^9K) well. Figure 2 shows the total RR rate coefficients of the present calculation together with the results of Landini and Monsignori Fossi (LM90)[18] and Arnaud and Rothenflug (1985) (AR85),[19] the present RR rate coefficients are consistent with the data of AR85 in lower temperature ($T = 10^4$–$10^{6.6}$K) and trend to fit with those of LM90 in higher temperature ($T = 10^6$–10^8K). Figure 3 shows the present CI rate coefficients and the data

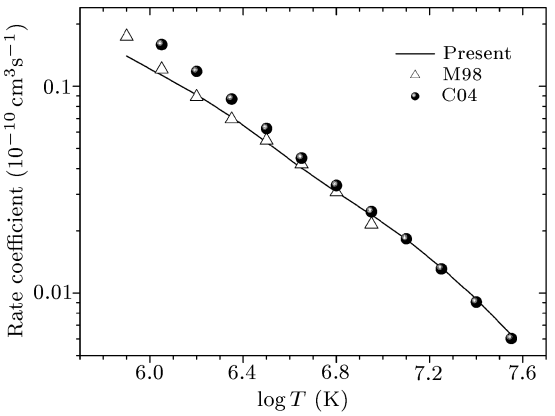

Fig. 1. The total DR rate coefficients of Al^{10+}.

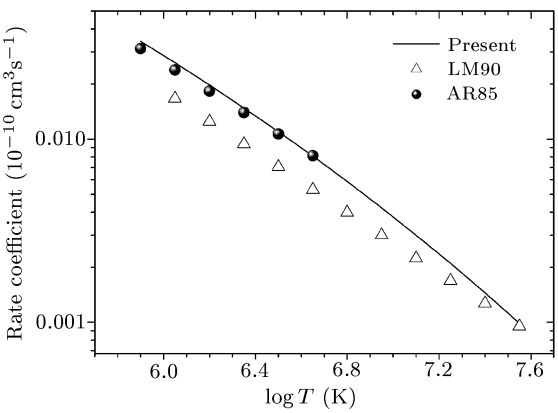

Fig. 2. The total RR rate coefficients of Al^{10+}.

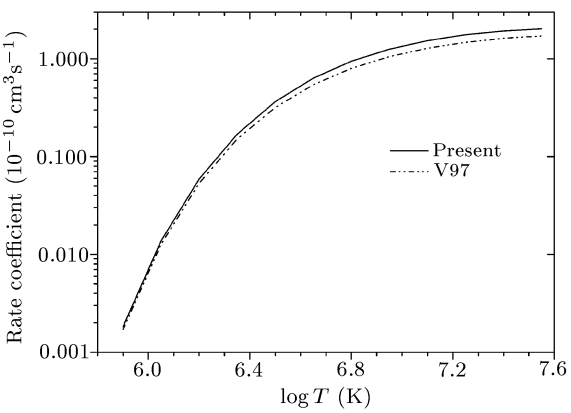

Fig. 3. The total CI rate coefficients of Al^{10+}.

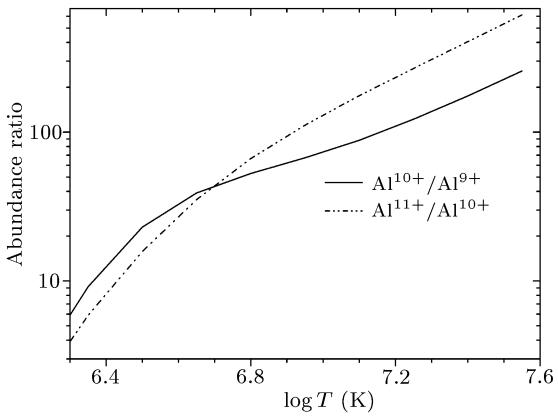

Fig. 4. Ionic fractional abundance.

of Voronov (V97).[20] Those two curves are accordant approximately.

Based on Eq. (6), the contributions of DR, RR, and CI to the line formation are also related to the fractional abundances of the charge states (Al^{9+}, Al^{10+}, and Al^{11+}), we calculate the fractional abundances of the three relevant ions in the CI equilibrium and plot the fractional abundance curves in Fig. 4.

In order to illustrate the contribution of the indirect processes, a ratio of the collective effects of DR+RR, RE (for Al^{10+}) to $3s$, $3p$, and $3d$ excited states relative to the direct CE is plotted in Fig. 5. It can be seen that the indirect processes are also important for total rate coefficients and generally more important for $3s$ and $3p$ states than $3d$ states in lower temperature, RE and DR+RR contributions reach 10%. Obviously, their contributions to the line emission cannot be ignored.

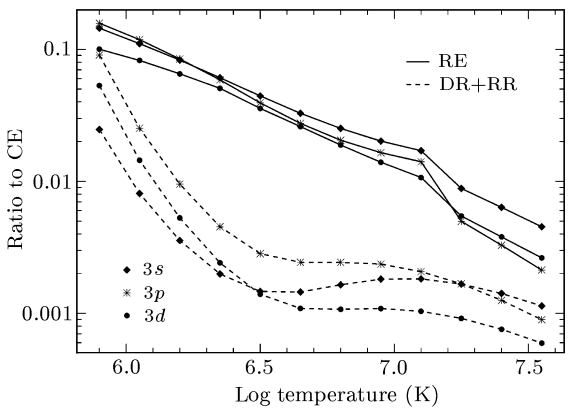

Fig. 5. Rate coefficients of indirect processes relative to direct CE for $3s$, $3p$, and $3d$ states.

Table 1. Line-formation rate coefficients of Al^{10+}.

I	log T	Coefficients (10^{-10}cm^{3}s^{-1})							
		RT	CE	RE	CE+CS3	CE+CS	RE+CS	DR+RR+CS3	DR+RR+CS
0	5.90	7.43×10^{1}	3.00×10^{-6}	2.89×10^{-1}	6.37×10^{-2}	7.43×10^{1}	3.08×10^{1}	1.02×10^{-2}	5.06×10^{-2}
0	7.55	3.31×10^{1}	3.42×10^{-7}	1.46×10^{-1}	1.76×10^{0}	3.31×10^{1}	2.08×10^{-1}	1.99×10^{-3}	7.72×10^{-3}
1	5.90	7.96×10^{8}	2.48×10^{1}	6.30×10^{-1}	2.49×10^{1}	2.49×10^{1}	6.39×10^{-1}	6.16×10^{-3}	8.07×10^{-3}
1	7.55	7.97×10^{8}	9.37×10^{0}	1.65×10^{-2}	1.01×10^{1}	1.02×10^{1}	1.89×10^{-2}	7.17×10^{-4}	1.48×10^{-3}
2	5.90	8.77×10^{8}	4.92×10^{1}	1.21×10^{0}	4.94×10^{1}	4.94×10^{1}	1.23×10^{0}	1.23×10^{-2}	1.62×10^{-2}
2	7.55	8.78×10^{8}	1.88×10^{1}	3.29×10^{-2}	2.02×10^{1}	2.05×10^{1}	3.76×10^{-2}	1.46×10^{-3}	3.13×10^{-3}
3	5.90	1.75×10^{11}	8.60×10^{-2}	1.27×10^{-2}	8.61×10^{-2}	8.78×10^{-2}	1.27×10^{-2}	1.10×10^{-3}	2.17×10^{-3}
3	7.55	1.73×10^{11}	5.27×10^{-1}	2.92×10^{-3}	5.27×10^{-1}	6.69×10^{-1}	3.03×10^{-3}	9.89×10^{-5}	7.62×10^{-4}
4	5.90	3.36×10^{11}	1.95×10^{-2}	3.38×10^{-3}	1.95×10^{-2}	2.15×10^{-2}	3.39×10^{-3}	1.10×10^{-3}	1.92×10^{-3}
4	7.55	3.38×10^{11}	5.35×10^{-1}	1.24×10^{-3}	5.35×10^{-1}	5.94×10^{-1}	1.27×10^{-3}	3.93×10^{-5}	5.11×10^{-4}
5	5.90	3.33×10^{11}	3.81×10^{-2}	6.63×10^{-3}	3.81×10^{-2}	4.21×10^{-2}	6.65×10^{-3}	2.19×10^{-3}	3.83×10^{-3}
5	7.55	3.36×10^{11}	1.06×10^{0}	2.43×10^{-3}	1.06×10^{0}	1.17×10^{0}	2.51×10^{-3}	7.79×10^{-5}	1.08×10^{-3}
6	5.90	9.93×10^{11}	5.46×10^{-2}	5.66×10^{-3}	5.46×10^{-2}	5.70×10^{-2}	5.69×10^{-3}	1.11×10^{-3}	3.03×10^{-3}
6	7.55	9.88×10^{11}	5.13×10^{-1}	1.50×10^{-3}	5.13×10^{-1}	5.79×10^{-1}	1.52×10^{-3}	1.58×10^{-5}	3.37×10^{-4}
7	5.90	9.91×10^{11}	8.17×10^{-2}	8.53×10^{-3}	8.17×10^{-2}	8.53×10^{-2}	8.57×10^{-3}	1.66×10^{-3}	4.53×10^{-3}
7	7.55	9.86×10^{11}	7.70×10^{-1}	2.29×10^{-3}	7.70×10^{-1}	8.69×10^{-1}	2.31×10^{-3}	2.37×10^{-5}	5.28×10^{-4}

In the calculation of indirect processes, cascade contributions are taken into account. Table 1 lists the contributions of cascade in these processes. In this table, energies are increased with the level sequence I going up, log T is the base 10 logarithm of the temperature in Kelvin, RT is the total depletion rate of the state in units of s^{-1}, CE and RE are the rate coefficients without cascade respectively, CE+CS, RE+CS and DR+RR+CS are the rate coefficients with all cascade contributions included, CE+CS3 and DR+RR+CS3 are the rate coefficients including only the cascade contributions from $n = 3$ states. All rate coefficients are in units of 10^{-10} cm^{3}s^{-1}. It can be seen that cascade is important for the lower levels from this table. Because we focus on the thin Al plasmas, ions almost occupy the lower levels, the cascade is not neglected.

When the electron density N_e is fixed to be 10^{10} cm^{-3}, based on the Lorentz lineshape, spectra emitted from Li-like aluminium plasma are simulated in the CI equilibrium in Fig. 6. The results are in good agreement with experiment[21] in the lineshape. To illustrate the contribution of the indirect processes, three different models including single-ion (Al^{10+}), double-ion (Al^{10+} and Al^{11+}) and three-ion (Al^{9+}, Al^{10+}, and Al^{11+}) are used corresponding to $N_{\rm ion} = 1$, 2, 3. In Fig. 6, plots in the same row have the same temperature but include different indirect processes. The first column includes only CE and the subsequent radiative cascades from Al^{10+}, the second column in-

cludes DR and RR from Al^{11+} as well, and the third column also includes the RE and CI effects and inner-shell excitation lines from Al^{9+}. Thus, different indirect processes contribute distinctly to emissive lines shape.

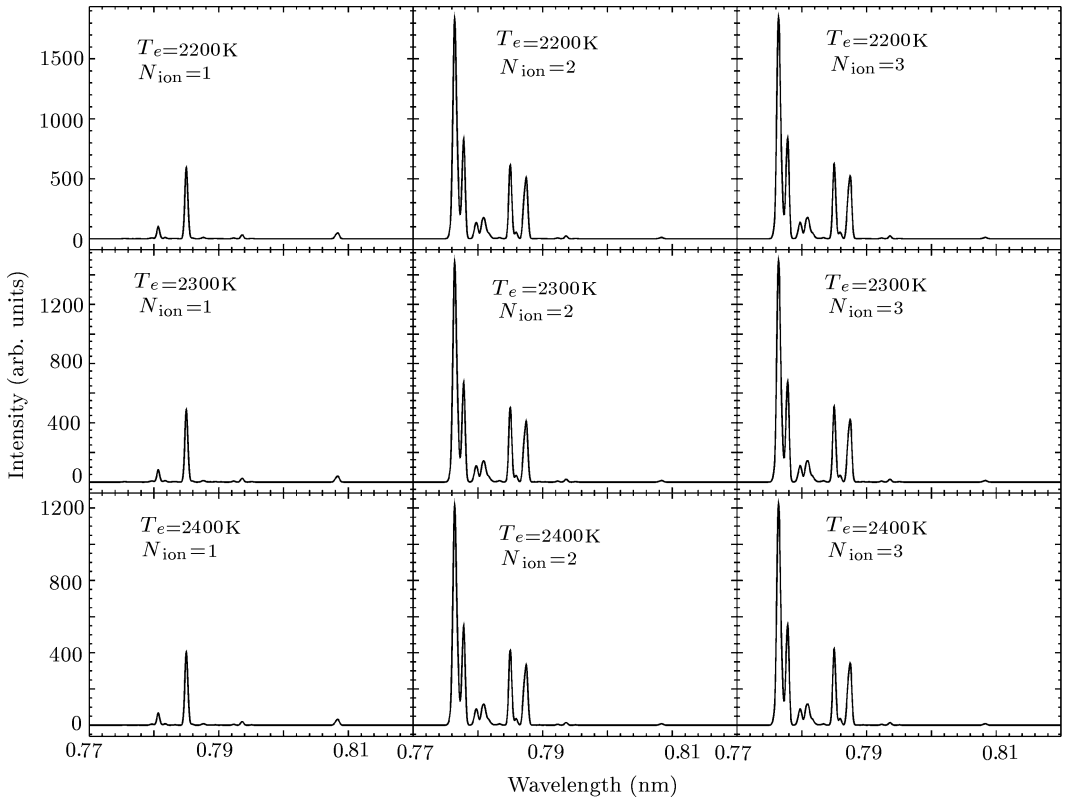

Fig. 6. Simulated spectra of Al ions.

In summary, the x-ray spectra from Li-like aluminium plasmas are synthesized by FAC, the systematic investigation of the role of indirect processes in the line formation is conducted. It is concluded that DR, RR, CI and RE are very important processes other than direct CE during the x-ray spectrum simulation for L-shell plasma of Li-like aluminium. In addition, cascade is not ignored in these processes.

References

[1] Burkhalter P G, Dozier C M and Nagel D J 1977 *Phys. Rev.* A **15** 700

[2] Burkhalter P G, Davis J, Rauch J, Dahlbacka G and Schneider R 1979 *J. Appl. Phys.* **50** 705

[3] Dunn J, Osterheld A L, Shepherd R, White W E, Shlyaptsev V N and Stewart R E 1998 *Phys. Rev. Lett.* **80** 2825

[4] Chase L E, Jordan W C, Perez J D and Pronko J G 1977 *Appl. Phys. Lett.* **30** 137

[5] Johnsonet D J, Kuswa G W, Farnsworth A V, Quintenz J P, Leeper R J, Burns E J T and Humphries S 1979 *Phys. Rev. Lett.* **42** 610

[6] Pang J Q, Wu Z Q, Yan J and Han G X 2004 *Chin. Phys. Lett.* **21** 2005

[7] Nishimura H, Kiso T, Shiraga H, Endo T, Fujita K, Sunahara A, Takabe H, Kato Y and Nakai S 1995 *Phys. Plasmas* **2** 2063

[8] Back C A, Kauffman R L and Bell P M 1995 *Rev. Sci. Instrum.* **66** 764

[9] Eidmann K, Andiel U, Pisani F, Hakel P, Mancini R C, Junkel-Vives G C, Abdallah J and Witte K 2003 *J. Quant. Spectrosc. Radiat. Transf.* **81** 133

[10] Zhang L Q, Han S S, Xu Z Z, Zhang Z Q, Fan P Z and Sun L 1995 *Phys. Rev.* E **51** 6059

[11] Duston D and Davis J 1980 *Phys. Rev.* A **21** 1664

[12] Perez J D and Payne G L 1980 *Phys. Rev.* A **21** 969

[13] Zeng J L, Zhao G and Yuan J M 2005 *Chin. Phys. Lett.* **22** 1972

[14] Gu M F 2003 *Astrophys. J.* **582** 1241

[15] Lucy L B 2001 *Mon. Not. R. Astron. Soc.* **326** 95

[16] Mazzotta1 P, Mazzitelli G, Colafrancesco S and Vittorio N 1998 *Astron. Astrophys.* **133** 403

[17] Colgan J, Pindzola M S and Badnell N R 2004 *Astron. Astrophys.* **417** 1183

[18] Landini M and Monsignori Fossi B C 1990 *Astron. Astrophys.* **82** 229

[19] Arnaud M and Rothenflug M 1985 *Astron. Astrophys.* **60** 425

[20] Voronov G S 1997 *At. Data Nucl. Data Tables* **65** 1

[21] Rosmej F B, Calisti A, Talin B, Stamm R, SüßW, Geißel M, Hoffmann D H H, Faenov A Ya and Pikuz T A 2001 *J. Quant. Spectrosc. Radiat. Transf.* **71** 639